Electronic behavior of selenium-rich selenium-tellurium liquid alloys

Shaw Shya Kao and Melvin Cutler
Department of Physics, Oregon State University, Corvallis, Oregon 97331-6507
(Received 18 March 1988)

A new method has been used to remove oxygen impurities from selenium, which has made it possible to make relatively reproducible measurements of the electrical conductivity σ and the thermopower S of Se-rich alloys. We report the results of a brief study of Tl_xSe_{100-x} alloys with $x \leq 4$ and a more extensive study of Se_xTe_{100-x} with x in the range of 50 to 100. The Tl-Se results provide quantitative evidence for the removal of oxygen impurities from Se, and a quadratic dependence of σ on x is found which supports a model for the electrical behavior based on the presence of diatomic $TlSe^-$ ions. Over much of the experimental range of composition and temperature in the Se-Te alloys, σ and S have a behavior which conforms to a model of transport by holes at the mobility edge of the valence band, with a minimum metallic conductivity σ_{c0} in the range from 10 to 40 $\Omega^{-1}\,cm^{-1}$. The transport data yield the distance of the Fermi energy E_F from the mobility edge E_{v1}. With the help of bond equilibrium theory for the effects of bond defects, it has been possible to separate the effects of T and x on E_F and E_{v1}, with the result that the large changes in $E_F - E_{v1}$ are found to be mostly due to changes in E_{v1} with x and T, rather than changes in E_F. At high T and at compositions approaching $x = 50$, where the Maxwell-Boltzmann approximation is poor because $E_F - E_{v1}$ is small, analysis based on Fermi-Dirac integrals yields quantitative evidence for the presence of a mobility edge, and a density of states which increases linearly with the hole energy. At $x \geq 80$, the thermopower falls off and goes through a maximum with decreasing T. This behavior is analyzed in terms of added transport at energies above E_{v1}, but it has not been possible to account for it in terms of the expected behavior of localized states in the valence-band tail, simple donor or acceptor band states, or states at the conduction-band edge.

I. INTRODUCTION

The electrical conductivity σ and the thermopower S of high-resistivity selenium-rich liquid-semiconductor alloys are quite strongly affected by the presence of small concentrations of impurities. One of them, oxygen, is particularly difficult to remove. Among the experimental difficulties attributable to the presence of small quantities of oxygen, are variable curves for electrical conductivity $\sigma(T)$ and thermopower $S(T)$ as a function of temperature T, depending on the method of preparation of the sample and the thermal history of the sample. Similar difficulties are found in the study of selenium or its alloys in the crystalline and amorphous states.

There have been many reports on the effects of oxygen and methods for purification of Se. Much of this work has been in relation to the properties of the amorphous or crystalline state.[1-8] Studies emphasizing the effects on liquid Se have been reported by Henkels and Maczuk,[9,10] and by Gobrecht and co-workers.[11,12] Se is a constituent in many alloy systems which are liquid semiconductors, and the effect of oxygen impurities in preventing reproducible measurements has apparently impeded the study of these alloys in the Se-rich composition ranges, where the conductivity is small enough to be affected by uncontrolled impurities.

The binary alloy Se-Te, in particular, is a key system, and we have been trying for a long time to obtain data in the Se-rich range suitable for analysis, in order to deduce information about the electronic structure. Several methods for purifying Se have been tried, including some methods reported in the literature as well as newly devised ones. None of them have succeeded in yielding reproducible data until we developed a method which depends on combining the oxygen impurity with a small amount of added aluminum, followed by distillation of the selenium. This method, called Al purification for brevity, reduces the apparent effects of uncontrolled impurities in liquid Se to a very significant degree. This has made possible a study of Se-Te alloys, which is the main subject of this paper.

Although we have not made a comprehensive study of the effects of oxygen, we think that it will be worthwhile to describe the concepts concerning the metallurgy of oxygen in selenium which have guided the interpretation of our experiments. This will be done in the next section, which describes the purification procedure. Our ability to measure the amount of oxygen in the samples has been very limited due to the special difficulties in trace analysis for this element. The main quantitative evidence for the removal of the oxygen from selenium is indirect. It comes from a series of thermoelectric measurements of Tl-Se alloys in a composition range 0–4 at.% Tl. We shall report these results and their interpretation in Sec. III, since they provide the main justification for the assessment of our results in terms of relatively oxygen-free Se. The main work is a study of the alloy system Se_xTe_{100-x} in the composition range $x = 50-100$ in which semiconductor behavior occurs, and the experimental results will be described in Sec. IV. In Sec. V

theoretical analysis of the results indicates that the dominant transport mechanism is Maxwell-Boltzmann (MB) transport in extended states at the mobility edge of the valence band. At the two extremes of the composition range, other mechanisms start to play a role. Near $x=50$, the Fermi energy approaches the mobility edge at high temperatures, and it is necessary to analyze the results in terms of expressions involving Fermi-Dirac (FD) integrals. In the Se-rich extreme, a change in shape of the thermopower curves occurs which indicates an increasing contribution to the transport from states at energies above the valence-band mobility edge, which we shall refer to as "additional" transport. We derive in Sec. V detailed information about the magnitude of the conductivity at the mobility edge and the behavior of the Fermi energy and the energy of the mobility edge as a function of temperature and composition. The overall implications of our results in relation to other work is discussed in Sec. VI.

II. PURIFICATION OF Se

At high temperatures, we expect much of the oxygen to be incorporated into the chain structure of liquid selenium, largely in the form of twofold bonded (2F) atoms (—O—) substituted in the Se chains, together with a number of other possible forms, such as one-fold bonded (1F) negative ions ($—O^{(-)}$), or SeO_2 molecular clusters which may form a 2F unit —(SeO)—O— or a 1F negative ion —(SeO)—$O^{(-)}$. Since SeO_2 has a much higher vapor pressure than Se, fractional distillation has been a frequently used method of purification. At low temperatures (i.e., near the melting point of Se), there is evidence that SeO_2 tends to precipitate out of liquid Se as a poorly soluble separate phase. Solid SeO_2 has a chain structure similar to Se, with 2F —(SeO)—O— units instead of —Se— units, so it seems possible that intermediate forms will occur at low temperatures in which clusters of the form $[—(SeO)—O—]_n$ accumulate within Se chains. As a result, the physical separation of SeO_2 may be erratic due to nucleation phenomena involving SeO_2 chain segments. This can account for some of the inconsistent behavior which is observed in the electrical and optical properties of the liquid.[13] Some purification procedures which have been used attempt to separate SeO_2 by precipitation at low temperatures.

Another approach for removing oxygen from selenium has been chemical reduction by carbon, ammonia, or hydrazine. These reactions are usually carried out at high temperatures ($>500\,°C$), but hydrazine reduction has been carried out at temperatures close to the melting point (219 °C). The efficacy of this approach depends in large measure on the difference in free energy of the two competing forms in which the oxygen can be bonded, i.e., H_2O or CO versus SeO_2. The Al-purification method is based on the consideration that aluminum oxide is much more stable than CO or H_2O at temperatures around 500 °C.

In our laboratory, a number of methods have been tried, including fractional distillation at 180 °C, distillation of Se at 500 °C combined with reduction by carbon at that temperature, and reduction with ammonia. None of these procedures have led to a sufficient improvement in the electrical properties of the liquid Se. The observed behavior is similar to what has been reported by other workers. The conductivity has two characteristics attributed to the presence of oxygen (1) Plots of $\ln\sigma$ versus $1/T$ generally have a lower temperature range in which the activation energy E_2 is considerably lower than the activation energy E_1 observed at higher temperatures. (2) The magnitude of $\sigma(T)$ is variable for different samples, and in some cases it is affected by the thermal history in the course of measurements. This variability is largest in the low-temperature part of the $\sigma(T)$.[11] The thermopower curves are subject to considerably more variability with sample and thermal history. The behavior is complicated by a more complex shape in S plotted against $1/T$. These curves have a positive slope at high T, and with decreasing T, S goes through a maximum and drops abruptly to negative values, where it tends to level off at still lower T. Depending on the sample, there is a large variation in the relative temperature ranges in which these three kinds of behavior occur, and in the maximum and minimum values of S at the two extremes of temperature also vary considerably.

The Al-purification procedure is carried out in a V-shaped fused quartz cell whose final shape is shown in Fig. 1. At the start, there is a constricted opening to a filling tube at the bottom of the right side. Commercial highly purified Se and a small amount of Al is added and transferred to the left side, after which the cell is sealed under a vacuum. The cell is then placed in a tube furnace at about 500 °C with a baffle separating the two parts of the cell at the narrow region. This makes it possible to maintain the empty compartment of the cell at a lower temperature, so that Se distills over to it within a few hours or overnight. Then the cell is cooled, and the purified sample is removed.

When the Se containing a small amount of Al is brought to a high temperature, we expect the Al to react with most of the oxygen which is present to form the very stable compound Al_2O_3, and the remaining Al will be in the form of aluminum selenide. On distillation of the Se, whose boiling point is 685 °C, the amount of Al and O which is transferred depends on the vapor pressures of atoms or molecules which may contain these elements. Diatomic AlO molecules are known to have a vapor pressure large enough to make spectroscopic measurements

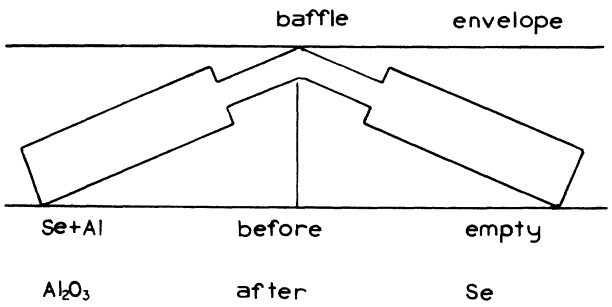

FIG. 1. Purification cell.

possible, and we expect diatomic AlSe molecules to have similar properties. In order to minimize the distillation of Al or O, we minimized the amount of excess Al, and kept the distillation temperature as low as possible, consistent with a reasonable distillation rate.

Trace analyses were made for Al and O in the purified samples. The Al concentrations were 40–70 ppm and the O concentrations were 600–1200 ppm. The latter values are in a similar range to concentrations for samples which had not been purified, or which had been purified by other methods. It is believed that the O found in the Al-purified samples resulted from moisture absorbed from the air through the walls of the polyethylene containers in which the samples were stored before the analysis.[14] The Al-purified samples are very hygroscopic and have a noticeable odor of H_2Se which forms from reaction with the moisture present in the air. The main evidence that we have succeeded in removing oxygen comes from the electrical properties of liquid-Se and Se-rich alloys with Te, Tl, and As, in which the effects attributed to the presence of oxygen, discussed earlier, are absent or markedly reduced. Quantitative information which specifically indicates that the changes are due to the removal of oxygen comes from an examination of thermoelectric data obtained for Tl-Se alloys, which is described in the next section.

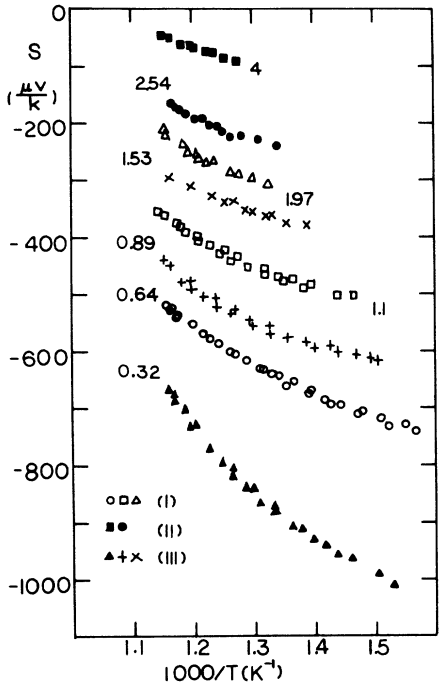

FIG. 3. S vs $1/T$ for Tl-Se alloys. Compositions are given in at. % Tl. The symbols indicate the compositions measured in three separate runs (I, II, and III.)

III. MEASUREMENTS OF Tl-Se

Measurements of $\sigma(T)$ and $S(T)$ were made on Tl_xSe_{100-x} alloys in the composition range 0–4 at. % Tl. There is a liquid-liquid phase separation at low temperatures, and the temperature range was from the liquid temperature up to about 610 °C. The results are shown in Figs. 2 and 3. Previous studies of Tl-Se in this composition range have been reported by Petit and Camp (σ only)[15] and by Rasolondramanitra and Cutler (σ and S).[16] In the latter work, which covered a much larger composition range (0–55 at. % Tl), the results for $x \leq 4$ were marred by poor reproducibility and irregularity of the curves for $\sigma(T)$ and $S(T)$. It now seems clear that this was caused by the presence of significant amounts of oxygen, which removed some of the Tl in the form of a relatively insoluble oxide. As a result, the amount of dissolved Tl within the electrode region of the cell depended on the sample and its thermal history. The present results obtained with Al-purified samples, shown in Figs. 2 and 3, are very reproducible and consistent.

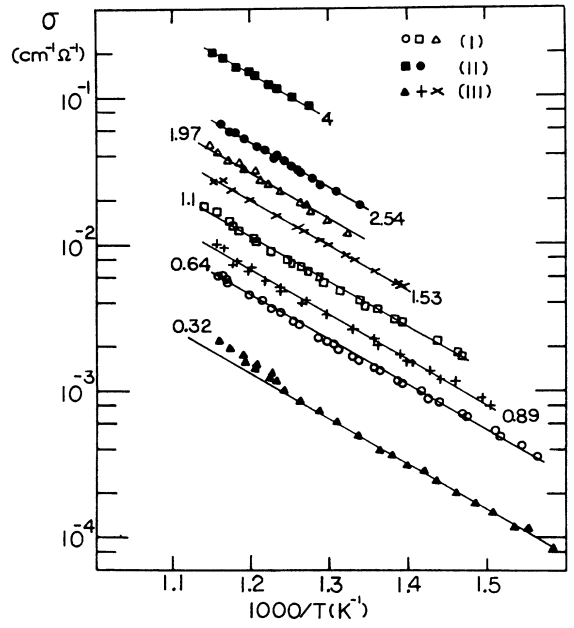

FIG. 2. Logσ vs $1/T$ for Tl-Se alloys. Compositions are given in at. % Tl. The symbols indicate the compositions measured in three separate runs (I, II, III.)

To test the hypothesis about the effect of oxygen, we have examined isothermal curves for the dependence of σ on x. For this purpose, it is very helpful to know the functional dependence of σ on x, so that a straight line can be obtained by plotting the appropriate function of σ. We have found empirically that σ varies a x^2, and therefore plotted $\sigma^{1/2}$ versus x. (There is a theoretical explanation for this dependence which is presented below.) The results are shown in Figs. 4 and 5 for alloys prepared with Se purified by fractional distillation, and Al-purified Se, respectively. It is seen in Fig. 4 that the line crosses the composition axis at 0.1–0.2 at. % Tl, which indicates removal of some of the added Tl by oxygen originally present to form a poorly soluble oxide. It is believed to be Tl_2O_3, in which case the original concentration of oxygen was >0.3 at. %. (This corresponds to 600 ppm.) The amount of Tl removed from the solution is seen to decrease with T, as one would expect because of an increased solubility of the oxide. For the Al-purified alloy,

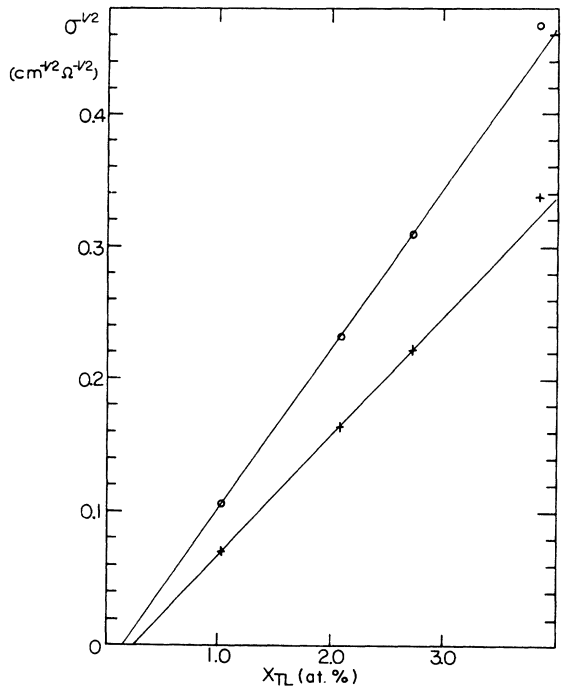

FIG. 4. $\sigma^{1/2}$ vs x at two temperatures for Tl-Se alloys in which the Se was purified by distillation at 180 °C. (○) indicates $T=833$ K, and (+) indicates $T=769$ K.

shown in Fig. 5, the line has a positive intercept, which corresponds to the electrical conductivity for pure Se.

The study in Ref. 16 showed that the electrical conductivity at low concentrations of Tl is mainly due to ionic transport attributed to diatomic $TlSe^-$ ions. The mobility of these ions is expected to be inversely proportional to the viscosity of the Se. Since most of the Tl atoms terminate Se chain molecules, and the viscosity of a mixture of long-chain molecules is proportional to their length,[16] the net result is that the ionic mobility should be proportional to the Tl concentration x. The concentration of the $TlSe^-$ ions is also expected to be proportional to x, thus explaining the observed relationship $\sigma \propto x^2$. This result provides further support for the ionic transport mechanism proposed in Ref. 16.

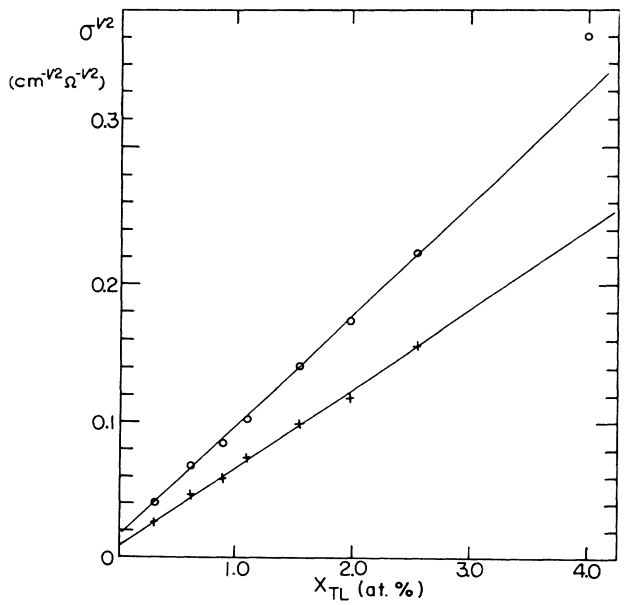

FIG. 5. $\sigma^{1/2}$ vs x at two temperatures for Al-purified Tl-Se alloys. (○) indicates $T=833$ K and (+) indicates $T=769$ K.

IV. MEASUREMENTS OF Se-Te ALLOYS

We report here measurements of Se_xTe_{100-x} in the composition range 50–100 at. % Se. The experimental procedures have been described in previous publications.[17,18] The measurements were carried out in a series of "runs." Each run consisted of a set of measurements of $\sigma(T)$ and $S(T)$ for a succession of compositions obtained by adding Te or Se to the previous composition. This resulted in at least four sets of measurements at compositions at intervals of 10 at. % Se between 50 and 100 at. % Se. In addition, a run was carried out which included compositions 85, 95, and 97 at. % Se. Representative curves are shown in Figs. 6 and 7.

As compared to earlier measurements, the results are much more reproducible at high-Se concentrations. The main sources of error are uncontrolled impurities (at $x>90$), thermocouple errors, and composition errors caused by distillation of Se. The uncontrolled impurities, believed to be due to sodium ions, led to a variation in S of about 200 μV/K in Se, but this dropped to 30 μV/K at $x=90$. These impurities may also be responsible for occasional variations in σ which could be as large as 30% in pure Se, but are much smaller in the alloys. Thermocouple errors create an uncertainty in S of about 5%. There is a composition error which is caused by a slow loss by evaporation of Se from the electrode region of the measurement cell.[17,18] This increases during the course of a run and showed up mainly in the values of σ at the Te-rich compositions, which were usually the last ones measured in the course of a run. This led to composition errors estimated to be as large as 1%. The data in Figs. 6 and 7 were taken from measurements made early in a run and thus are subject to little error due to distillation.

The present results are similar to those obtained previously in this and other laboratories, particularly at the Te-rich end of the composition range.[12,19,20] But we note a qualitative difference in that the previous curves for $\ln\sigma$ and S versus $1/T$ at $x \leq 70$ showed an abrupt change in slope, whereas the present curves in the same temperature range have at most a very gradual change in slope for $\ln\sigma$ and no change in slope for S. The change in slope of S has been interpreted as evidence of transport in an acceptor band, in addition to the transport which occurs primarily in the valence band.[19] In our analysis of the transport data in the next section, we find no evidence of a significant contribution to transport from the acceptor band in this range of T and x. However, as we show in a related paper,[21] analysis of the electronic behavior at $x<50$ leads to evidence that the acceptor band merges with the valence band in that composition range, causing a distinct effect on the behavior of σ. At $x \geq 80$ the $S(T)$

curves tend to level off at low T. This seems to be due to an increasing contribution to transport from states at energies above the mobility edge.

V. INTERPRETATION OF Se-Te BEHAVIOR

A. Maxwell-Boltzmann region

The transport parameters σ and S are derived from the $\sigma(E)$, the conductivity of states at energy E using the phenomenological equations

$$\sigma=\int\sigma(E)(-df/dE)dE\ , \tag{1}$$

$$S=(k/e)\int\sigma(E)[(E-E_F)/kT](df/dE)dE\ , \tag{2}$$

where $f(E)$ is the Fermi-Dirac (FD) factor $\{1+\exp[(E-E_F)/kT]\}^{-1}$. The magnitude and the sign of the thermopower indicates that the distance of the Fermi energy E_F above the energy of the electronically conducting states $\gg kT$ except for $x=50$ and 60 at high temperatures. Therefore the Maxwell-Boltzmann (MB) approximation can be used in the transport equations for σ and S. Assuming that $\sigma(E)$ drops abruptly to zero at valence-band mobility edge energy E_{v1}, the expressions for σ and S are

$$\sigma_v=\sigma_c(1+a_1+a_2+\cdots)\exp[(E_F-E_{v1})/kT]\ , \tag{3}$$

$$S_v=(k/e)[(E_F-E_{v1})/kT+1+A_c]\ , \tag{4}$$

where $\sigma_c=\sigma(E_{v1})$.[22] [A more explicit description of the model for $\sigma(E)$ is given in Sec. V C.] We have introduced the subscript v to distinguish these results from other transport mechanisms to be considered later. The parameters $a_n=(kT)^n(d^n\ln\sigma/dE^n)$ and

$$A_c=(a_1+2a_2+3a_3+\cdots)/(1+a_1+a_2+a_3+\cdots) \tag{5}$$

are correction terms evaluated at $E=E_{v1}$. They correct for change in $\sigma(E)$ from $\sigma(E_{v1})$ in a range of energies $\approx kT$ below E_{v1}. In this section, we shall use the zeroth-order approximation in which a_n and A_c are zero. Later, we shall include the first-order correction a_1.

At a given value of x and T, experimental values of σ and S can be used to calculate σ_c and E_F-E_{v1}. Solving Eqs. (3) and (4) gives

$$\sigma_{c0}=\sigma\exp[(Se/k)-1]\ , \tag{6}$$

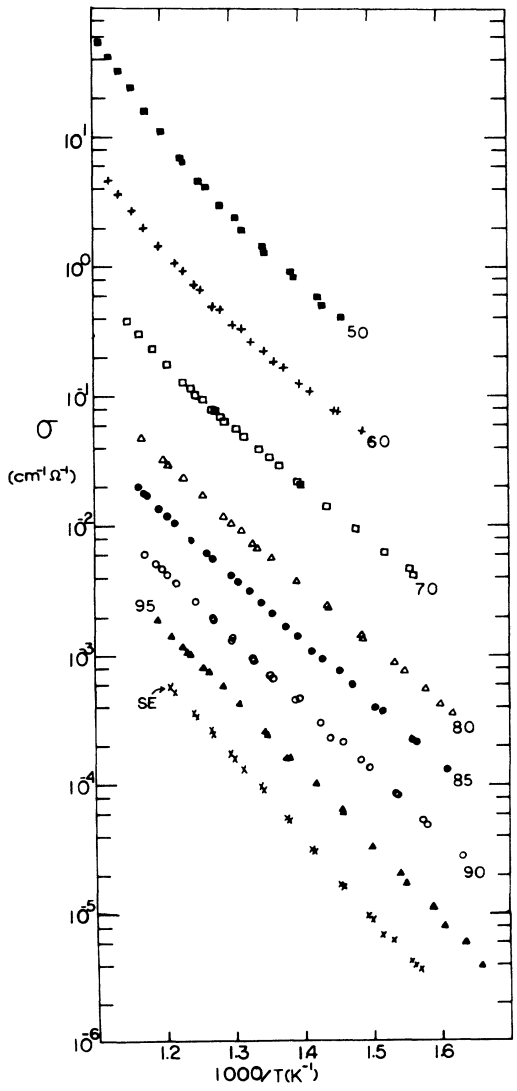

FIG. 6. Logσ vs $1/T$ for Te-Se alloys. Compositions of the alloys are given in at. % Se.

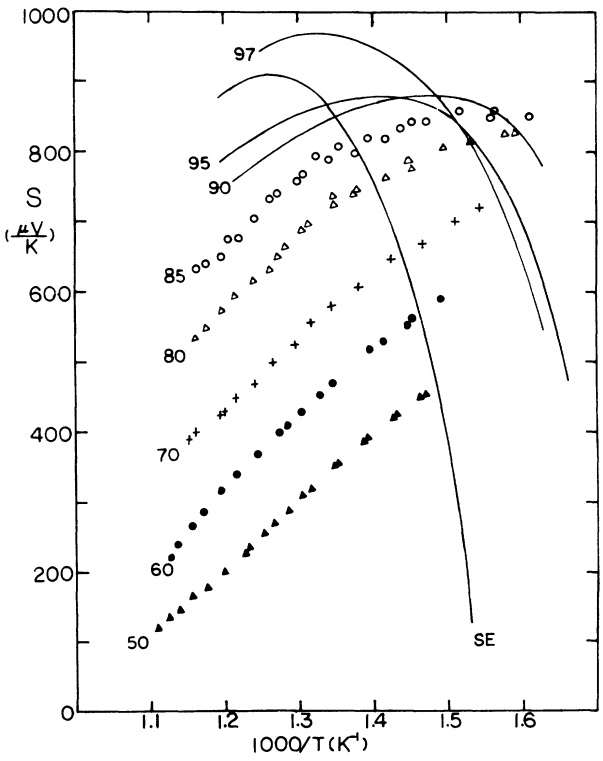

FIG. 7. S vs $1/T$ for Te-Se alloys. Compositions of the alloys are given in at. % Se. To avoid confusion, results for Se-rich compositions are in the form of smoothed curves.

where the subscript 0 indicates that the correction parameters a_n are taken to be zero. In Fig. 8 we show the dependence of σ_{c0} on T for various compositions in a typical run. It is seen that σ_{c0} for a given composition is nearly independent of T except at high T for values of x approaching 50, and at low T for large values of x. The values of σ_{c0} in different runs varied by as much as a factor 2 because of the great sensitivity of Eq. (6) to the errors in S.

The large changes in σ_{c0} with T at small x are due to failure of the MB approximation, and a more appropriate analysis of the behavior in this region in terms of Fermi-Dirac (FD) integrals is presented in Sec. V B. The large changes with T at large x are attributed to additional transport by states at energies above the mobility edge, which is discussed in Sec. V D. For the data not affected by these two phenomena, σ_{c0} is in the range 10–50 $\Omega^{-1}\,\mathrm{cm}^{-1}$. In Fig. 9 we show plots of E_F-E_{v1} obtained from the thermopower with Eq. (4) (with $a_n=0$) in regions of x and T where the simple MB expression is valid. For $x>70$, where the thermopower curves are affected by the additional transport, E_F-E_{v1} is calculated from the σ data in a manner which is explained in Sec. V D.

B. The Fermi-Dirac region

When E_F-E_{v1} is comparable to kT or negative, it is necessary to take into account the detailed curve $\sigma(E)$ when integrating Eqs. (1) and (2). $\sigma(E)$ can often be described by a power law, and the effect of the mobility edge is to cause σ to drop to zero abruptly over a range of E small compared to kT. Thus we describe $\sigma(E)$ by the model

$$\sigma(E)=C(E_{v0}-E)^s \quad \text{if } E<E_{v1}\ ,$$
$$=0 \quad \text{if } E>E_{v1}\ , \tag{7}$$

where C and s are parameters to be determined empirically, and E_{v0} represents the edge of the valence band including the localized states. Substituting Eq. (7) into Eqs. (1) and (2) leads to expressions involving definite integrals which we refer to as extended FD integrals:

$$G_n(\alpha,x_c)=\int_{x_c}^{\infty}\frac{x^n\exp(x-\alpha)}{[1+\exp(x-\alpha)]^2}dx\ , \tag{8}$$

where $\alpha=(E_{v0}-E_F)/kT$ and $x_c=(E_{v0}-E_{v1})/kT$. The ordinary FD integral $F_n(\alpha)$ is equal to $G_{n+1}(\alpha,0)/(n+1)$.[23]

For the case where there is no mobility edge, i.e., $E_{v0}-E_{v1}\ll kT$,

$$\sigma=sC(kT)^{s-1}F_{s-1}(\alpha) \tag{9}$$

and

$$S=(k/e)[-\alpha+(s+1)F_s(\alpha)/sF_{s-1}(\alpha)]\ . \tag{10}$$

The value of s is determined by comparing an experimental plot of $\log(\sigma T^{-s})$ versus S with the theoretical curve calculated by setting α in Eqs. (9) and (10) to various

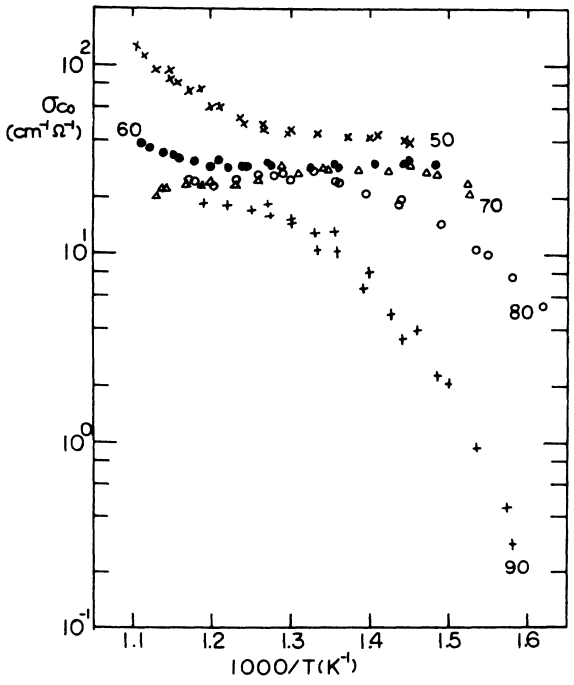

FIG. 8. Plots of σ_{c0} vs T^{-1} for various compositions obtained from Eq. (6).

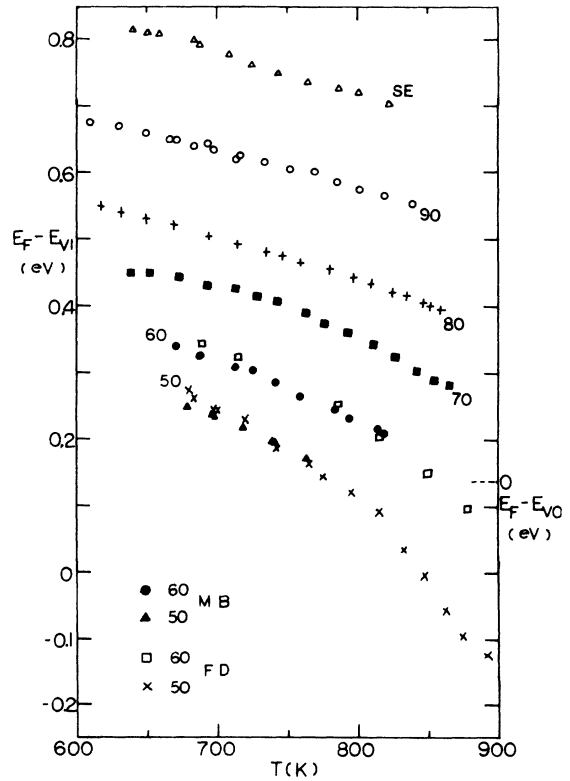

FIG. 9. Plots of E_F-E_{v1} vs temperature at different compositions x. Data for $x\geq 80$ were calculated from Eq. (3) with the preexponential factor equal to 11 $\Omega^{-1}\,\mathrm{cm}^{-1}$. Data for $x\leq 70$ marked MB were calculated from Eq. (4) with $a_n=0$, and those marked FD were calculated from Eq. (10).

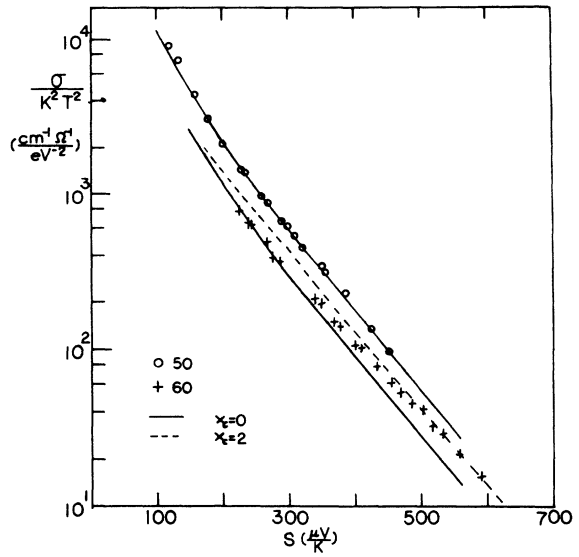

FIG. 10. Fit of theoretical and experimental Fermi-Dirac transport curves for $x=50$ and 60. The theoretical curves were obtained from Eqs. (9) and (10) with $s=2$ and values of C given in Table I.

values. The theoretical curve should overlap the experimental curve when it is shifted vertically by an amount corresponding to the value for sCk^{s-1}. For the two compositions $x=50$ and 60 which are in the FD range, a good match was found with $s=2$, as is shown in Fig. 10. This value for s is in agreement with the value found for the more metallic compositions $x=30$ and 40, and corresponds to a density of states $N(E)$ which is linear in E.[21] The values of C obtained in this procedure are listed in Table I.

A small deviation between the theoretical and experimental curve for $x=60$ can be seen in Fig. 10. This is due to a finite mobility edge, i.e., $E_{v0}-E_{v1}\geq kT$. A procedure for determining $E_{v0}-E_{v1}$ which alters Eqs. (9) and (10), so as to incorporate extended FD integrals with $x_c>0$, is insensitive because the effect of the mobility edge is small. This can be seen from the small shift of the dashed curve in Fig. 10, which was calculated for $x_c=2$. A much better procedure for determining $E_{v0}-E_{v1}$ is to evaluate E_F-E_{v0} as a function of T from experimental data for S, using Eq. (10), and compare this curve with E_F-E_{v1} obtained from Eq. (4) in the MB range. In Fig. 9 we show that the two curves overlap very well for $x=50$ and 60, assuming in both cases that $E_{v0}-E_{v1}=0.14$ eV.

TABLE I. Mobility-edge data of Se_xTe_{100-x}.

x	50	60	70	80	90
σ_c (Ω^{-1}cm^{-1})	10	5			
σ_{c0} (Ω^{-1}cm^{-1})	45	35	13	11	11
C (Ω^{-1}cm^{-1}eV^{-2})	449	259			
E_{v1} (eV)	0.14	0.14			
a_1 ($T=770$ K)	0.835	0.961			
$R(a_1)$	2.90	3.20			
σ_{c0}/σ_c	4.5	7.0			

This value of $E_{v0}-E_{v1}$, together with the values C listed in Table I yield values $\sigma_c=C(E_{v0}-E_{v1})^2$ of 10 and 5 Ω^{-1}cm^{-1}, respectively, for $x=50$ and 60. These are considerably smaller than the corresponding values 45 and 35 Ω^{-1}cm^{-1} for σ_{c0} obtained from Eq. (6), using data for which the MB approximation is valid. This discrepancy can be resolved by including the first-order correction a_1. Then Eqs. (3)–(5) yield a correction factor

$$R(a_1)=\sigma_{c0}/\sigma_c=(1+a_1)\exp[a_1/(1+a_1)]\ . \tag{11}$$

This correction can be applied only approximately because T, and hence a_1, varies by a factor ≈ 1.5 over the experimental range. This correction is applied for $x=50$ and 60 in Table I, where $d\sigma/dE$ in a_1 is calculated from $2CE_{v1}$, as inferred from the expression for $\sigma(E)$. The rough agreement between $R(a_1)$ and σ_{c0}/σ_c seems reasonable in view of the wide scatter in experimental values of σ_{c0} between runs.

We also list in Table I the values of σ_{c0} obtained for $x\geq 70$. They can also be expected to be larger than the true σ_c. But we have no reliable basis for making a correction, since there is no assurance that the value of a_1 remains the same when the composition is changed.

C. Temperature dependence of E_F and E_{v1}

The general behavior of σ and S in Figs. 6 and 7 indicates that E_F approaches the valence-band edge as T or Te concentration is increased, and this process is described quantitatively in Fig. 9. The question arises why it does so. In early work on Se-Te alloys[12,20,24] it was believed that the position of E_F is determined by the excitation of electron-hole pairs across the band gap, and the decrease in E_F-E_{v1} reflects a decrease in the size of the band gap. In order to explain the absence of an ambipolar effect on S due to the electrons, it was necessary to assume that the electrons are much less mobile. It is now generally believed, however, that the value of E_F is determined by charge balance between ionic-bond defects: $1F$ negative D^- and $3F$ positive D^+ ions.[25,26] In the case of a solid, the Fermi energy is pinned between the donor and acceptor bands whose empty states correspond to the D^+ and D^- ions, respectively. In the case of a liquid, the equilibrium situation is described somewhat differently, because the filled states of the two bands which correspond to neutral paramagnetic $1F$ D^* and $3F$ D^0 centers, respectively, change their concentrations with T or x independently of the D^+ and D^- centers. The appropriate equations have been derived in a bond equilibrium theory (BET), which takes into account the statistical effects due to the presence of the bond-defect atoms in the chainlike molecular structure.[27,28] The concentrations d_i of these defects D_i are given by the equations

$$d^*=p_1\exp(-g^*/kT)\ , \tag{12}$$

$$d^0=p_3\exp(-g^0/kT)\ , \tag{13}$$

$$d^- = p_1 \exp[-(g^- - \varepsilon_F)/kT] , \quad (14)$$

$$d^+ = p_3 \exp[-(g^+ + \varepsilon_F)/kT] , \quad (15)$$

where g_i ($=e_i - Ts_i$) is the free energy of formation of a D_i center from the normally bonded atom,[29] and ε_F is the distance of E_F from a reference energy E_R. The concentrations are normalized to the concentration of atoms N_a ($\approx 2.7\times 10^{22}$ cm^{-3}). p_n is the "polymer factor" associated with the effect of the formation of an n-fold bond-defect atom on the molecular-chain statistics.

The value of E_F is obtained by equating d^- and d^+:

$$E_F = E_R + (g^- - g^+)/2 + \tfrac{1}{2}kT \ln(p_3/p_1) . \quad (16)$$

The reference energy E_R is the energy of the state in the electron band structure from which an electron is removed in forming a D^- ion, or to which an electron is added when a D^+ ion is formed. The values of g^+ and g^- depend implicitly on the value of E_R. This point is important because if one chooses E_R to have an arbitrary convenient value (say E_{v1}), the values of g^+ and g^- will be coupled to the changes in E_{v1} with x and T. It will be convenient in our discussions to think of E_R as the center of the valence band in pure Se, and we shall consider changes in E_{v1} with respect to this reference energy due to changes in x and T.

A method for separating the effects of T and x on the two parameters in the experimentally determined $E_F - E_{v1}$ is provided by the use of Eq. (16) in conjunction with experimental data for the spin density d_s derived from magnetic susceptibility measurements.[30] There is reason to believe that $d^* \gg d^0$ over the range of those measurements,[31] so that d_s is equal to d^* in Eq. (12). The experimental data show an activation energy for $x > 50$ which is nearly independent of x. Therefore, the shifts in the curves with x reflect changes in the value of p_1. The values of p_1 and p_3 depend on the branch ratio R_b, the average number of chain branches per molecule, which is determined by the relative concentrations of $3F$ and $1F$ bond defects. In this experimental range, $R_b \gg 1$, so that $p_1 \propto R_b$ and $p_3 \propto R_b^{-1}$.[27] Using this information, we derive from Eqs. (12) and (16)

$$E_F(x) - E_R = \text{const} - kT \ln d^*(x) . \quad (17)$$

This equation, together with experimental data for the isothermal dependence of d^* on composition allows us to determine the changes in E_F with x and T independently of the changes in E_{v1}.[32]

In Fig. 11, we show curves for $E_F(x) - E_F(100)$ versus T, calculated from Eq. (17) with data in Ref. 30. Using this information together with the data in Fig. 9, we derive curves for $E_{v1}(x) - E_{v1}(100)$ versus T which are shown in Fig. 12. Two things are to be noted. The changes with temperature in Figs. 11 and 12 are small compared with Fig. 9. That means that the temperature coefficients are nearly the same as for $x = 100$. The temperature coefficient of $E_F(100)$ can be estimated from Eq. (16) and data in Ref. 30, and the result is $dE_F(100)/dT = -1.9\times 10^{-4}$ eV/K. That, together with the temperature coefficient of $E_F - E_{v1}$, gives

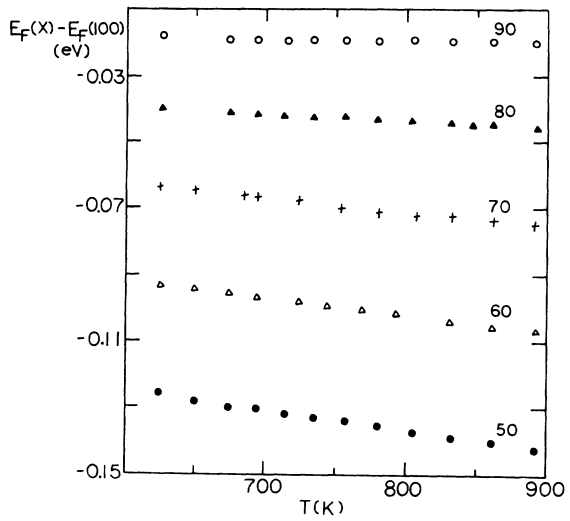

FIG. 11. Plots of $E_F(x) - E_F(100)$ vs T for various compositions x.

$dE_{v1}(100)/dT = 4.1\times 10^{-4}$ eV/K. Thus we see that the major part of the decrease of $E_F - E_{v1}$ with T is due to an increase in E_{v1}, and this is nearly independent of x. The second thing to notice is the dependence of the magnitudes of E_F and E_{v1} on composition. The increase in E_F from $x = 50$ to $x = 100$ is about 0.13 eV, whereas E_{v1} decreases about 0.4 eV in the same composition range. So our results are consistent with the concept that the Fermi energy is nearly pinned by the ionic-bond defects. Thus we arrive at the interesting conclusion that the large changes in σ and S in the direction of metallic behavior as x is decreased and T is largely due to an upward motion of the mobility edge of the valence band, rather than a downward shift of E_F.

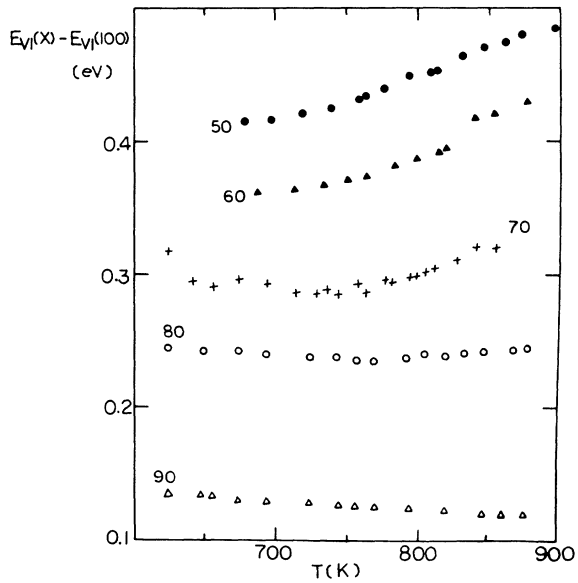

FIG. 12. Plots of $E_{v1}(x) - E_{v1}(100)$ vs T for various compositions x.

D. Transport in states above E_{v1}

At $x \geq 80$, the thermopower curves in Fig. 7 show an increasing tendency to level off and decrease with decreasing T. This indicates that states at energies above E_{v1} are contributing to the transport at low T in addition to the transport at the mobility edge. At the same time, there is no abrupt decrease in slope of $\log\sigma$ versus T^{-1} at low T in Fig.6, as would be expected if there is a substantial shift of transport to the states at $E > E_{v1}$. Therefore these contributions represent a small fraction of σ.

The most obvious possible contributors to this transport are (1) localized states in the tail of the valence band above the mobility edge, (2) acceptor-band states, (3) donor-band states, and (4) conduction-band states (localized and extended). For convenience, we shall refer to these four groups of states as "bands." To consider these possibilities, Eqs. (1) and (2) are rewritten in the form

$$\sigma = \sigma_v + \sum_i \sigma_i \tag{18}$$

and

$$\sigma S = \sigma_v S_v + \sum_i \sigma_i S_i \ , \tag{19}$$

where i can take the values L, A, D, or C for the four cases described above. S_i can be related to the energy E_i of the conducting states by

$$S_i = (E_F - E_i)/eT \ . \tag{20}$$

E_i is an average band energy defined by

$$E_i = \int E_j [\sigma(E_j)/\sigma_i](-df/dE_j)dE_j \ , \tag{21}$$

where E_j is restricted to the states in band i and σ_i is obtained from Eq. (1) with the integration likewise limited to the band i.

It will be useful to derive equations which are expressed in terms of the fractions $F_i = \sigma_i/\sigma$ of the transport contributed by these four different bands, since the absence of a large change in slope in the $\ln\sigma$ curves indicates that the fraction of transport at the mobility edge $F_v = \sigma_v/\sigma$ does not become small compared to one. From Eq. (6) we get

$$S_v = S_{v0} - (k/e)\ln F_v \ , \tag{22}$$

where

$$S_{v0} = (k/E)[\ln(\sigma_{c0}/\sigma) + 1] \ . \tag{23}$$

Starting with an assumed value for σ_{c0}, one can calculate S_{v0} from experimental data for σ. If $\sum_i F_i \ll 1$, then $S_{v0} \approx S_v$, and one can make a good estimate for $E_F - E_{v1}$ by using Eq. (3) (with $a_n = 0$). That is the way the curves in Fig. 9 were calculated for $x \geq 80$, where the ambipolar contributions cause S to deviate strongly from S_v.

Using Eqs. (18)–(23), one can derive the following useful equation:

$$S_{v0} - S = \sum F_i (E_i - E_{v1})e/T + L(F_v) \ . \tag{24}$$

$L(F_v)$ is a correction term which is relatively small unless $F_v \ll 1$:

$$L(F_v) = (k/e)(\ln F_v + 1 - F_v) \ . \tag{25}$$

For instance, $-L(F_v) < 17\ \mu\text{V/K}$ if $F_v > 0.5$.

We show in Fig. 13 plots of $S_{v0} - S$ versus $1/T$ for compositions $x \geq 80$. For $x \leq 90$, the values for σ_{c0} were chosen to fit the data in the high-T regions, where the constant positive slope indicates that $F_v = 1$. In each case, a good fit was obtained with $\sigma_{c0} = 11\ \Omega^{-1}\text{cm}^{-1}$. For $x > 90$, where the thermopower curves in Fig. 7 do not have a distinctly linear segment at high T, we somewhat arbitrarily chose the same value for σ_{c0}. The error in the choice of σ_{c0} is expected to have the largest influence at high T, where $S_{v0} - S$ is smallest.

There is not enough information to distinctly separate the contributions of F_i and $E_i - E_{v1}$ in Eq. (24), but interesting limiting relations can be obtained. The fact that $F_i \leq 1$ allows us to use the data in Fig. 13 to set lower limits on the values of $E_i - E_{v1}$. Using the points at the lowest T, which correspond to the largest values of $E_i - E_{v1}$, we arrive at values, listed in Table II as $E_{\max}$, which range from 0.076 eV for $x = 80$, to 0.79 eV for $x = 100$. Since the localized band-tail states are expected to lie within ≈ 0.2 eV of the mobility edge, they cannot account for the added transport for the larger values of x. Although some contributions to σ from σ_L cannot be ruled out, we shall continue the discussion in terms of the possible dominant contribution from a single band, which may be the acceptor, donor, or conduction band.

Assuming that one band dominates the sum in Eq. (24), and ignoring the relatively small term $L(F_v)$, we multiply the equation by σeT and rearrange it to get

$$\sigma_i = \sigma(S_{v0} - S)eT/(E_i - E_{v1}) \ . \tag{26}$$

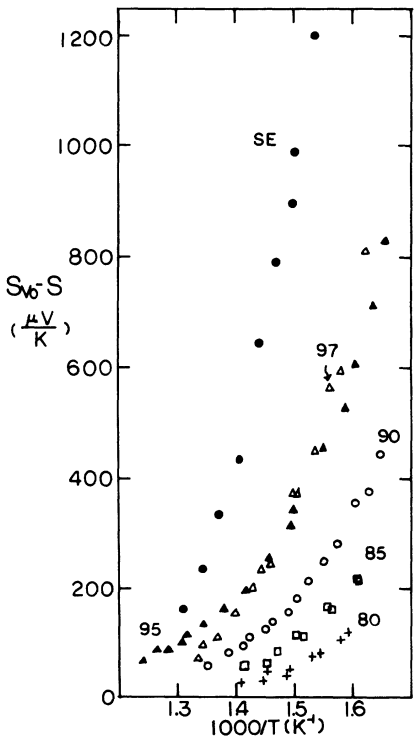

FIG. 13. Plots of $S_{v0} - S$ vs $1/T$ for compositions $x \geq 80$.

TABLE II. Energy of ambipolar transport in Se_xTe_{100-x}.

x	E_{max} (eV)	$E(\sigma_1)$ (eV)	$E(\sigma_v)$ (eV)	E_{k0} (eV)	$E_{K0}-E(\sigma_1)-E(\sigma_v)$ (eV)
80	0.076	0.246	0.928	1.97	0.80
85	0.132	0.400	0.946		
90	0.271	0.505	1.051	2.02	0.45
95	0.502	0.689	1.143	2.16	0.33
97	0.500	0.546	1.161		
100	0.786	0.554	1.234	2.20	0.41

The value of E_i-E_{v1} is not known, but we know that it depends weakly on T and is smaller than the mobility gap energy, which is estimated to be ≈ 2.0 eV.[33] To get a good approximation to the temperature dependence of σ_t and the rough magnitude, we have calculated approximate values, called σ_1, by assuming that $E_i-E_{v1}=1$ eV. After removing some erratic points at the highest T where $S_{v0}-S$ is relatively small, these are plotted in Fig. 14. Except for $x=80$, these curves have well-defined activation energies, listed in Table II, which are less than 0.7 eV. These values are apparently too small to be consistent with acceptor, donor-, or conduction-band transport. The reasons for this conclusion are presented in the remainder of this section.

σ_C is given by an expression like Eq. (3):

$$\sigma_C=\sigma_{cn}\exp[-(E_{c1}-E_F)/kT] , \tag{27}$$

so that the sum of the activation energies for σ_C and σ_v should be equal to the mobility gap $E_{c1}-E_{v1}$ at $T=0$.

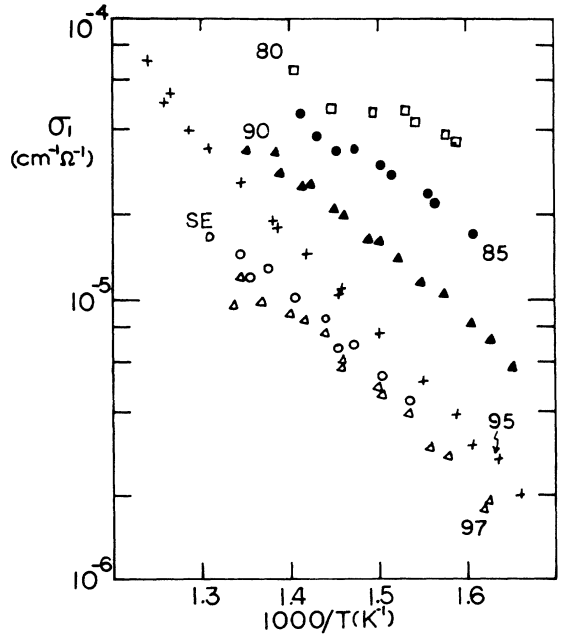

FIG. 14. Approximate behavior of the ambipolar contribution to σ are shown in plots of $\ln\sigma_1$ vs $1/T$ for $x\geq 80$. The calculated activation energies $E(\sigma_1)$ are given in Table II.

The latter can be obtained from optical data by Perron[33] for E_{K0}, the optical-band gap at $T=0$, which are listed in Table II. We also list the activation energies for σ, which is essentially the same as σ_v. It is seen that $E(\sigma_1)+E(\sigma)$ falls short of the optical-band gap by at least 0.3 eV.

The conductivities of the acceptor and donor bands are closely related. Assuming that the states are localized, an expression for the acceptor band can be written

$$\sigma_A=(e^2L^2h/3kT)[N_a d^- d^*/(d^-+d^*)] , \tag{28}$$

where h is a hopping frequency and L is the distance between acceptor sites:

$$L=[6/\pi N_a(d^-+d^*)]^{1/3} . \tag{29}$$

An expression for σ_D is obtained by replacing d^- by d^+ and d^* by d^0. The hopping frequency contains a factor $\exp(-2\alpha L)$, where α is the attenuation factor for a wave function at an acceptor site. If $d^- \gg d^*$, these equations imply that the activation energy of σ_A is

$$E(\sigma_A)=e^*+(\tfrac{2}{3})(\alpha L-1)e_I-\langle kT\rangle , \tag{30}$$

where e^* is the energy of formation of a D^* center and $e_I=(e^-+e^+)/2$ is the energy of formation of a single ion. If $d^- \ll d^*$, e^*, and e_I are interchanged in Eq. (30). Magnetic susceptibility data show that $e^*=0.68$ eV,[30] and there is information from optical measurements which indicates that $e_I\approx 0.6$ eV in liquid Se.[34] Therefore, if $E(\sigma_A)$ is to be consistent with $E(\sigma_1)$ it is necessary that $\alpha L\approx 1$. However this is precluded by the magnitude of σ_1, which is so small as to require that $\alpha L\gg 1$. Therefore, σ_1 cannot be identified with σ_A.[35]

Similar arguments eliminate donor-band transport as a possibility. Since $d^-=d^+$, they have the same activation energy e_I. The activation energy e^0 of D^0 centers is not known. It can be estimated from the observation that $d^0<d^*$ in Se at $T>800$ K.[30,31] Therefore e^0 is not greater than e^*. But e^0 cannot be too much smaller than e^*, otherwise d^0 would exceed d^* in spite of the smaller prefactor ($p_3 \ll p_1$) in Eqs. (12) and (13). Estimates of p_1 and p_3 (Ref. 31) suggest that $e^*-e^0\leq 0.3$ eV. This leads to the same conclusion as for the acceptor-band mechanism: The activation energy of σ_1 requires that $\alpha L\approx 1$ but the magnitude requires that $\alpha L\gg 1$.

We have presented arguments that no one of the four proposed mechanisms can account for extra transport above the valence-band mobility edge. Can it be explained by a combination of more than one of these

mechanisms? It seems not, since they all require a larger activation energy than what is observed in σ_1, and a combination of these mechanisms would likewise have an activation energy which is too large.

VI. SUMMARY AND DISCUSSION

In summary, the Al-purification method had made possible much more reproducible thermoelectric measurements of Se-rich alloys. A brief study of Tl_xSe_{1-x} alloys has been presented which provides indirect quantitative evidence of removal of oxygen from Se and has yielded more precise information about transport in the composition range $x<0.04$. A quadratic dependence of σ on x has been found which provides additional support for a previously advanced model of transport by $(TlSe)^-$ ions.

The main experimental study yields much-improved data for S and σ in Se_xTe_{100-x} in the range $x \geq 50$, which provides quantitative information about the valence-band mobility edge and the position of the Fermi energy. Over a broad range of T and x, the Maxwell-Boltzman approximation to the transport equations yields directly numerical values for σ_c and E_F-E_{v1}. In the near-metallic region, analysis with the help of Fermi-Dirac integrals has yielded quantitative information about $\sigma(E)$, including an estimate of the energy at which the mobility edge occurs. In the Se-rich alloys, a downward curvature of the thermopower curves has been analyzed in terms of transport contributions from states above E_{v1}. The analysis shows difficulties in attributing this transport to any of the four most likely mechanisms: localized band-tail states above E_{v1}, acceptor band, donor band, or conduction band. Finally, with the help of equations of bond-equilibrium theory, it has been possible to separate the contributions of E_F and E_{v1} to the changes of E_F-E_{v1} with x and T. We find that E_F stays relatively constant, while E_{v1} increases strongly with T and x.

The small deviation of the points at large S from the theoretical curve in Fig. 10 seems to be the most direct evidence yet found for the existence of a mobility edge in a liquid semiconductor. The values of σ_c of ≈ 10 $\Omega^{-1}\text{cm}^{-1}$ are rather small, and Mott's formula[36,37] $\sigma_C=0.032\pi e^2/hL_i$ implies an inelastic scattering length $L_i \approx 60$ Å. This seems rather large for a liquid. It may be that the model used for $\sigma(E)$ in Eq. (7) is too simplified to give reliable information on this point. Aside from the corrections a_n which have been taken into account in part, the overall treatment of transport, starting with Eqs. (1) and (2), may be over idealized in that it neglects contributions of inelastic-scattering processes.[38]

The mechanism for the additional transport described by the curves in Fig. 14 remains a puzzle. The well-defined activation energies for the curves for $x>80$ suggests strongly that the mechanism involves charge centers with a well-defined energy. One possibility seems to be a donor or acceptor band based on dipole pairs (D_P centers), i.e., D^+ and D^- ions which are directly bonded to each other.[39] The estimated value of the energy e_I to form an ion is smaller than the Coulomb energy of a D^+-D^- ion pair at the distance of closest approach. Consequently these D_P centers may have higher densities than the simple D^+ or D^- ions. Of course, the failure to find an acceptable model for the additional transport may also result from a more fundamental inadequacy of the theory. It may be that the transport reflects a more complicated phenomenon which is not adequately described by Eqs. (1) and (2). One thing which makes us suspect that this may be the case is that the downward curvature in the thermopower curves (Fig. 7) is not accompanied by any detectable upward curvature in the curves for $\log\sigma$ (Fig. 6). This is hard to explain in the framework of Eqs. (1) and (2).

Finally, we would like to discuss what seems to be the most interesting result of this work, the fact that the large changes in S and σ with x and T are mainly due to shifts of the valence-band mobility edge E_{v1} with respect to an invariant reference energy E_R, which we take to be the center of the valence band in Se. This explanation for the change in the transport behavior seems roughly similar to the earliest interpretation of the transport changes in terms of a smearing out of the pseudogap with decreasing x and increasing T. But now we are led to consideration of much more specific mechanisms. The curves in Fig. 12 indicate that E_{v1} increases about 0.4 eV between $x=100$ and $x=50$. The valence band is derived from the outermost p orbitals of the chalcogen atoms and is the result of broadening of the band due to mutual interaction of the lone-pair electrons which are not used in making bonds. Atomic calculations show that the $(5p)^4$ state of the Te atom is 0.934 eV higher than the $(4p)^4$ state of the Se atom.[40] We know of no theoretical calculations of the effect of alloying on the width of the lone pair band in Se-Te alloys. But it seems reasonable to suppose that a 50% mixture of Te atoms would cause the upper edge of the Se band to increase by half of this amount, which agrees roughly with the rise in E_{v1}.[41] The large value of dE_{v1}/dT presumably is caused by thermal broadening of the valence band, for which, again, there does not yet seem to be any available theory.

ACKNOWLEDGMENT

This research has been supported by the National Science Foundation under Grant No. DMR-83-20547.

[1]F. Eckart, Ann. Phys. (Leipzig) **14**, 223 (1954).
[2]F. Eckart, Ann. Phys. (Leipzig) **17**, 84 (1956).
[3]F. Eckart, Phys. Status Solidi **2**, K23 (1962).
[4]P. T. Kozyrev, Fiz. Tverd. Tela (Leningrad) **1**, 113 (1959) [Sov. Phys.—Solid State **1**, 102 (1959)].
[5]G. B. Abdullaev, G. M. Aliev, Kh. G. Barkinkhoev, Ch. M. Askerov, and L. S. Larionkina, Fiz. Tverd. Tela (Leningrad) **6**, 1018 (1969) [Sov. Phys.—Solid State **6**, 786 (1964)].

[6]G. B. Abdullaev, S. I. Mekhtieva, D. Sh. Abdinov, and G. M. Aliev, Phys. Status Solidi **11**, 891 (1965).
[7]F. B. Gadzhiev, Fiz. Tekh. Poluprovodn. **7**, 977 (1973) [Sov. Phys.—Semicond. **7**, 663 (1973)].
[8]V. A. Twaddell, W. C. Lacourse, and J. D. Mackenzie, J. Non-Cryst. Solids **8-10**, 831 (1972).
[9]H. W. Henkels, J. Appl. Phys. **21**, 725 (1950).
[10]H. W. Henkels and J. Maczuk, J. Appl. Phys. **24**, 1056 (1953).
[11]H. Gobrecht, D. Gawlik, and F. Mahdjuri, Phys. Kondens. Mater. **13**, 156 (1971).
[12]H. Gobrecht, F. Mahdjuri, and D. Gawlik, J. Phys. C **4**, 2247 (1972).
[13]R. A. Burley, Phys. Status Solidi **29**, 551 (1968).
[14]We are grateful to Dr. W. Ehemann of the University of Kentucky for his help in the trace analysis of oxygen.
[15]R. B. Petit and W. J. Camp, Phys. Rev. Lett. **35**, 182 (1975).
[16]H. Rasolondramanitra and M. Cutler, Phys. Rev. B **29**, 5694 (1984).
[17]M. Cutler, *Liquid Semiconductors* (Academic, New York, 1977), Chap. 4.
[18]H. Rasolondramanitra and M. Cutler, Rev. Sci. Instrum. **55**, 602 (1984).
[19]M. Cutler and H. Rasolondramanitra, J. Non-Cryst. Solids **61-62**, 1097 (1984).
[20]J. C. Perron, Adv. Phys. **16**, 657 (1967).
[21]S. S. Kao and M. Cutler, Phys. Rev. B **37**, 10 581 (1988).
[22]M. Cutler and N. F. Mott, Phys. Rev. **181**, 1336 (1969).
[23]M. Cutler, Ref. 17, p. 201.
[24]N. F. Mott, Philos. Mag. B **24**, 1 (1974).
[25]M. Cutler, *Amorphous and Liquid Semiconductors* (University of Edinburgh, Edinburgh, 1977), p. 833.
[26]N. F. Mott and E. A. Davis, *Electronic Processes in Non-Crystalline Materials,* 2nd ed. (Clarendon, Oxford, 1979), p. 544.
[27]M. Cutler, Phys. Rev. B **20**, 2981 (1979).
[28]M. Cutler, Philos. Mag. B **47**, 11 (1983).
[29]There is an implicit assumption here that these free energies are the same for Te and Se atoms. The general behavior of $E_F - E_{v1}$ is consistent with this assumption.
[30]J. A. Gardner and M. Cutler, Phys. Rev. B **20**, 529 (1979).
[31]M. Cutler and W. G. Bez, Phys. Rev. B **23**, 6223 (1981).
[32]In deriving Eq. (17), we have neglected the entropy terms in g^+ and g^-, which would otherwise contribute terms proportional to T.
[33]J. C. Perron, J. Non-Cryst. Solids **8-10**, 272 (1972).
[34]F. G. Bell and M. Cutler, Phys. Rev. B **34**, 5270 (1986).
[35]We have not included a hopping activation energy in the hopping frequency because its value is unknown and is expected to be of the order of kT. Inclusion of this in the discussion would increase the discrepancy.
[36]N. F. Mott, J. Non-Cryst. Solids **77-78**, 115 (1985).
[37]N. F. Mott, Philos. Mag. B **52**, 169 (1985).
[38]D. Belitz and W. Schirmacher, J. Phys. C **16**, 913 (1973).
[39]M. Cutler and H. Rasolondramanitra, in *Localization and Metal-Insulator Transitions,* edited by H. Fritzsche and D. Adler (Plenum, NY, 1985), p. 119.
[40]F. Herman and S. Skillman, *Atomic Structure Calculations* (Prentice Hall, Englewood Cliffs, NJ, 1963).
[41]N. F. Mott (private communication) has pointed out to us that the appropriate formula for the conductivity at the mobility edge in a highly disordered liquid is $\sigma_c = g_c^2 \sigma_B$, where σ_B is the band conductivity and $g_c \approx \frac{1}{3}$. In view of this, the conclusion that the states near the top of the band are derived from the Te atoms offers a reasonable explanation for the excessively small values of σ_c, discussed above, in terms of an effective value of σ_B which is small because of the low concentration of Te atoms from which the states near the mobility edge are derived.